COUPLED SIMULATION OF A THERMOELECTRIC GENERATOR APPLIED IN DIESEL ENGINE EXHAUST WASTE HEAT RECOVERY

by

Guo-Quan XIAO [*] ***and Zheng ZHANG***

School of Mechanical and Automotive Engineering, South China University of Technology, Guangzhou, China

Original scientific paper
https://doi.org/10.2298/TSCI181112322X

This work develops a heat transfer model of a thermoelectric generator to explore the coupled relationship between high temperature exhaust flows, structure, and the external cooling air. The coupled heat transfer results showed that the fins reached a uniform high temperature, for the rated speed, the average temperature is 474 K. The coupled design scheme of the thermoelectric generator tested by installing it in a 4-cylinder turbocharged Diesel engine exhaust system. Comparison of the test and simulation results showed that as engine speed increased, the inlet and outlet exhaust temperatures of the thermoelectric generator exhibited a parabolic trend increase. The cooling water outlet temperature and the top, middle, and bottom fin temperatures increased linearly, and the coupled model was verified. From idle speed to rated speed, the top, middle, and bottom fin temperatures increased from 458 K to 476 K, 417 K to 463 K, and 406 K to 449 K, respectively; the cooling water outlet temperature increased from 293.6 K to approximately 303 K. Hence, the thermoelectric components installed in fins can experience temperature differences of over 100 K, the heat transfer efficiency can increase which ensures consistent output performance of the thermoelectric generator based on coupled design between the heat exchanger and thermoelectric modules array column.

Key words: *thermoelectric generator, coupled design, waste heat recovery, Diesel engine*

Introduction

According to statistics, only about one-third of the heat emitted by engine combustion is generally converted to effective work. Two-thirds of the engine's fuel combustion energy is lost and diffused as heat, and 40% of the heat is discharged into the atmosphere in the form of engine exhaust [1, 2]. Among various waste heat recovery techniques, the thermoelectric generator (TEG), which can directly convert heat into electricity *via* the Seebeck effect of semiconductor materials, is one of the most promising given its simplicity, ruggedness, silent operation, and absence of compression-expansion moving parts and working fluid [3-5]. Although thermoelectric conversion technology to recover waste heat is an effective way to save engine energy [6], TEG's conversion efficiency has historically been much lower than conventional power generation devices. With an average exhaust temperature of 823 K and

* Corresponding author, e-mail: megqxiao@scut.edu.cn

the mass-flow rate of 480 g/s, the TEG system constructed by Zhang *et al.* [7] generated 1002.6 W electricity with a 2.1% heat-to-electricity efficiency. The maximum output power of 944 W for TEG applications in automobiles was reported by Liu *et al.* [8]. Relatively low thermoelectric conversion efficiency has limited TEG's development and application; however, thermoelectric power generation technology still receives considerable scholarly attention, namely due to engine exhaust acquisition at virtually no cost. Regarding TEG applications in engine waste heat recovery, determining how to improve thermoelectric generation efficiency continues to constrain engine exhaust recovery technology. There are three key technologies that have been found to improve thermoelectric generation efficiency [9]: continuous research and development of more high-performance thermoelectric materials, strengthening heat transfer, and optimizing thermoelectric conversion circuit. These methods can improve the heat transfer efficiency of TEG based on existing thermoelectric materials, and the efficiency can be increased by increasing the temperature difference between hot and cold thermoelctric junctions and, accordingly, extending the range of TEG operating temperatures. In practice, the maximum efficiency value will be lower, according to approximate calculations (14-18%), which is consistent with the data presented by Shtern [10]. The engine exhaust TEG includes high-temperature exhaust, structure, and the external cooling air. Heat transfer mainly includes convection and radiation heat transfer of high temperature exhaust, heat conduction, and radiation heat transfer of structures (*e. g.*, heat exchanger and thermoelectric element), and convection heat transfer of the cooling water system [11].

Hendricks [12] established and optimized a heat transfer model of thermoelectric generation and explored its guiding functions related to design. Using FLEXPDE software, Lazard [13] analyzed the effects of thermal properties on the Thomson effect and nonlinearity in TEM given the temperature distribution of the TEG module. Descombes and Boudigues [14] established a waste heat recovery system model and studied factors influencing the efficiency of waste heat recovery of gas turbines under a complex cycle. Chen *et al.* [15] studied the irreversible change process of TEG from an energy perspective and established a 3-D model of non-linear flow-thermoelectric coupling in a thermoelectric conversion system, which only considered the heat conduction equation. Ren *et al.* [16] calculated radiation on the outer surface of the power supply using the Carlo method and constructed the function relation of the external wall surface temperature and surface heat dissipation; the result was used as a generalized source term to combine the node network method and control volume method to conduct a coupling simulation internally in the thermoelectric generation supply. Zhang *et al.* [17] and Zhang and Ding [18] explored convection-radiation coupling and fluid-solid coupled heat transfer characteristics of a built-in TEG.

As indicated, previous studies have focused largely on simulating exhaust waste heat recovery in TEG systems performance. Researchers have begun to explore the design of coupled heat transfer in waste heat generators. It is well known that numerical simulation, as an important research method, can be used to directly evaluate device performance and provide suggestions for design optimization in a short research cycle. Weng and Huang [19] empirically investigated the effects of heat exchanger length and thermoelectric module coverage on automobile exhaust TEG system performance. Hsiao *et al.* [9] established a mathematical model of TEG modules applied to an automobile, but they simplified the TEG system into a thermal resistance network. Deng *et al.* [20] focused on the structural design of heat exchange attached to the TEG module. Hashim *et al.* [21] presented a model for the geometry optimisation of thermoelectric devices in a hybrid photovoltaic/thermoelectric (PV/TE) system. He *et al.* [22] presented a thin plate exchanger used in the TEG system, but the TEG modules were

not modeled and investigated in their work. Tian *et al.* [23] assumed that the per-TE unit performance in automobile exhaust TEG systems was the same; however, for a TEG module applied to an automobile, the exhaust flow in the automobile pipe and the coolant flow in the heat sink were unidirectional.

Royale and Simic [24] pointed out that a comprehensive investigation of TEG technological limitations, new TEG design and development, and corresponding simulations and testing are essential to future research. Meng *et al.* [25] developed a multiphysics TEG model for automobile exhaust waste heat recovery in which the exhaust was modeled as the actual heat source with a water-cooling heat sink as the cold source. Convective heat transfer, heat conduction, and electrical conduction were solved simultaneously, but the convective and radiant heat transfer between the heat exchanger, TEG module, and external cooling air were not. Because the convective and radiant heat transfer in the external cooling air was inherently coupled with heat conduction and electrical conduction in the TEG module, the determined inlet/outlet temperatures using the aforementioned method were inaccurate, resulting in a significant deviation in the predicted output power of TEG. To avoid this issue, an alternative approach is to develop a coupled heat transfer model in which convective and radiant heat transfer between the heat exchanger, TEG module, and external cooling air are solved simultaneously with heat conduction and electrical conduction in thermoelectric materials. To this point, however, a similarly coupled model for engine exhaust TEG systems has not been discussed in the literature.

In this paper, a coupled heat transfer model of a thermoelectric generation system is established that includes high temperature exhaust, structure, and the external cooling air. Using the established model, the coupled heat transfer effect is investigated under various engine operating conditions, and the coupled design scheme of TEG is defined and tested. Finally, the coupling design of the heat exchanger, TEG module, and external cooling air is realized by executing the coupled heat transfer model.

Coupled heat transfer model

This model is devised based on theoretical analysis of the efficiency of the waste heat power generator combined with existing thermoelectric materials and technological conditions.

Structural model

Authors are obliged to use System International (SI) for units (including non-SI units accepted for use with the SI system) for all physical parameters and their units.

The structure of TEG designed for diesel engine exhaust waste heat recovery is shown in fig. 1.

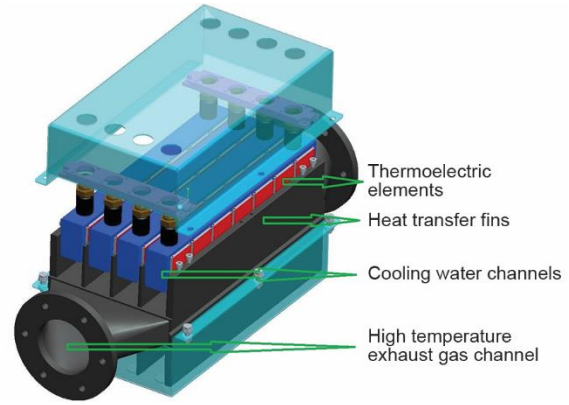

Figure 1. Thermoelectric generator structure

It mainly includes a high temperature exhaust channel, cooling water channels, heat transfer fins, and thermoelectric elements. It is used for performance analysis in the present study.

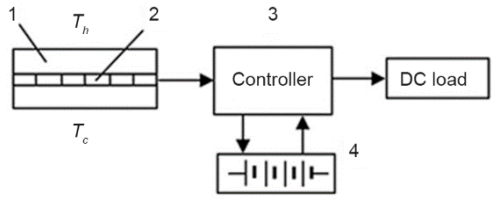

Figure 2. Thermoelectric generation system; *1 – heat exchanger, 2 – TEM array, 3 – controller, 4 – battery, T_h – high temperature, T_c – low temperature*

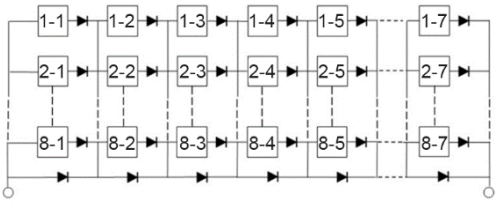

Figure 3. The TEM array based on SP structure

A thermoelectric generation system is composed of a heat exchanger, TEM array, battery and controller, which including DC-DC, maximum power point tracking, and charge-discharge controller. The relationship among them is depicted in fig. 2.

The high temperature exhaust from the inlet into the four high-temperature exhaust channels is separated by five heat-exchanging fins, and the five heat transfer fins extending up and down the channel form eight parallel cooling water channels. In total, there are 112 TEM pieces across 16 rows and 7 columns up and down the two layers. The fins in each layer are longitudinally divided into two symmetrical intervals (left and right), and the connection mode of TEM in each interval is as follows: first, the four pieces with same temperature difference are connected in a parallel group; second, seven of those groups in a row are connected sequentially as an SP sub-circuit. In addition, to prevent energy consumption, each group in the series is connected in parallel with a reverse bypass diode; to prevent circulation, each SP sub-circuit is connected sequentially with anti-diodes. Then, the two layers up and down form a 4×7 TEM array as shown in fig. 3.

Mesh model

The 3-D and middle sectional grid of the TEG are shown in fig. 4.

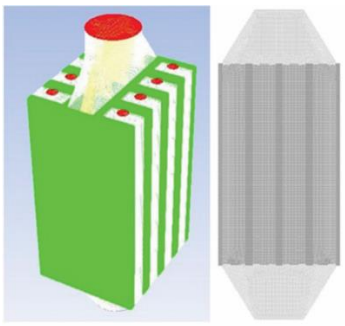

Figure 4. Thermoelectric generator 3-D and middle sectional grid

First, hypermesh is used to generate a quadrilateral mesh, then a six-side structured grid is generated for a total grid of 1.20, 1.82, 2.45, and 4.86 million elements, respectively. Regarding mesh skewness, the mesh is less than 0.6 and the body grid is less than 0.8.

Governing equations

The numerical model of the engine exhaust TEG system established in this work includes the flow equation, energy equation, and electric potential equation. The following assumptions are adopted in this model:

– the flow is single-phase, incompressible, and steady,
– gravitational force is ignored, and
– electric and thermal contact resistances are ignored.

Conjugate heat transfer simulations are carried out using FLUENT, which solves the equations:

$$\frac{\partial}{\partial x}(\rho u\phi)+\frac{\partial}{r\partial r}(r\rho v\phi)+\frac{\partial}{r\partial\theta}(\rho w\phi)=\frac{\partial}{\partial x}\left|\Gamma_\phi\frac{\partial\phi}{\partial x}\right|+\frac{\partial}{r\partial r}\left|r\Gamma_\phi\frac{\partial\phi}{\partial r}\right|+\frac{\partial}{r^2\partial\theta}\left|\Gamma_\phi\frac{\partial\phi}{\partial\theta}\right|+s_\phi \quad (1)$$

where ϕ is the flow parameter and Γ_ϕ – the diffusion coefficient. When $\phi = 1$, $\Gamma_\phi = 0$, eq. (1) is the equation of continuity. When $\phi = u, v, w$, $\Gamma_\phi = \mu$, eq. (1) are the equations of $x, r,$ and θ directional momentum, and when $\phi = k, \varepsilon$, $\Gamma_\phi = \mu_e/\sigma_k$, μ_e/σ_ε is the k-ε equation. When $\phi = C_p, T$, $\Gamma_\phi = \mu_e/\sigma_h$, eq. (1) is equation of energy, S_ϕ is source items of heat exchanger.

Numerical methods

The finite volume method is used to discrete the control equations, and the flow and heat transfer boundary-layer of the fluid-solid coupling interface uses the standard wall function. The turbulence model includes the standard two equations, and the pressure and velocity coupling of the discrete equations adopt a simple algorithm. Heat conduction and convective heat transfer are, respectively, described by thermal conductivity and the convective convection coefficient. The radiation heat exchange employed the discrete ordinates model, and ignores solar radiation. The second-order upwind scheme style is adopted, and the remainder of the energy equation convergence standard is less than 10^{-6}; all other items are less than 10^{-3}.

In order to reduce the effect of elements number on accuracy, the 3-D grid-independence was verified before formal calculation. The simulation model is divided into four different numbers of elements and calculated separately, the results of the calculations are given in tab. 1.

Table 1. Assessment of 3-D grid independence

Numbers of elements (million)	1.20	1.82	2.45	4.86
T_{hot} [°C]	256.7	253.5	245.8	244.6
T_{cold} [°C]	24.1	24.4	25.2	25.8
ΔT [°C]	232.6	231.1	220.6	218.8

According to the calculation results of T_{hot}, T_{cold}, and ΔT in different numbers of elements, the 2.45 million elements has been able to get a stable solution, so choose it as the computational meshes, and the second-order upwind scheme style and convergence standard are reasonable.

Boundary conditions

In terms of rated operating conditions, for the exhaust, a uniform mass-flow of $M_{g,in} = 0.55$ kg/s maintained at $T_{g,in} = 593$ K is set as the inlet boundary condition. For the coolant, the inlet velocity is $M_{w,in} = 0.70$ kg/s, and the inlet temperature is $T_{w,in} = 293.6$ K. At the exhaust and coolant channel outlets, the pressure is $p_{out} = 0.10$ MPa. The working fluid is assumed, respectively, to be ideal air and water for the exhaust and coolant channel; regardless of the reaction and composition of exhaust and water, their properties are listed in tab. 2. On the interfaces between the channel and solid wall, the velocity, temperature, and heat flux are continuous.

Table 2. Thermophysical properties of fluids

Materials	ρ [kgm^{-3}]	Cp [Jkg^{-1}K^{-1}]	λ [Wm^{-1}K^{-1}]	μ [kgm^{-1}s^{-1}]
Water	997	4179	0.613	0.000855
Air	1.161	1007	0.026	–

For the TEG module, the exhaust pipe and fins are made of aluminum alloy, the initial temperature is 300 K, and the convective heat transfer coefficient of the shell and atmosphere is 15 W/mK. All thermoelectric element material properties used in this study are listed

in tab. 3. Temperature dependent material properties are not reported in the literature, so the constant properties assumption is adopted here.

Table 3. Thermoelectric elements material parameters used in this study

Material	Seebeck coefficient [μVK^{-1}]	Electric resistivity [μΩm]	Heat conductivity coefficient [Wm^{-1}K^{-1}]
PbTe	–160	0.0015	2.8
BiTe (N)	–170	0.001	1.2
BiTe (P)	+180	0.00076	1.4

The pipe wall is set to conduct (heat conduction). The constant current and zero electric potential are, respectively, specified to the current inlet and outlet. Except for the current inlet and outlet, the current cannot flow out of the other outside surfaces of the TEG module, hence $\vec{J} \times \vec{n} = 0$ is specified for these surfaces with *n* denoting their normal direction. On the internal interface between any two adjacent materials, the temperature and heat flux are assumed to be continuous.

Results and discussion

Coupled heat transfer results

In this section, simulations are carried out for the grid mode and operation conditions of the system described in previous chapter with the material properties described in tabs. 1 and 2. The coupling heat transfer characteristics of the TEG at 100% load under various operating conditions are obtained, and the pressure, velocity, and fin coupling temperature of the middle section of the TEG under rated operating conditions are shown in figs. 5-7.

As shown in figs. 5 and 6, with high temperature exhaust through the internal high temperature channel in the TEG, the speed and pressure in the expansion section are reduced along the streamwise direction due to blocking effect from the three middle heat transfer fins in

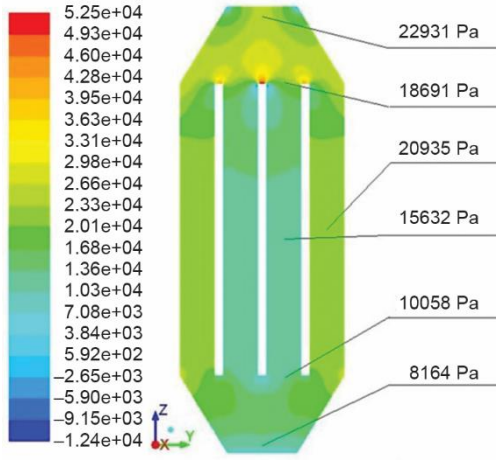

Figure 5. Middle sectional pressure of the TEG (*for color image see journal web site*)

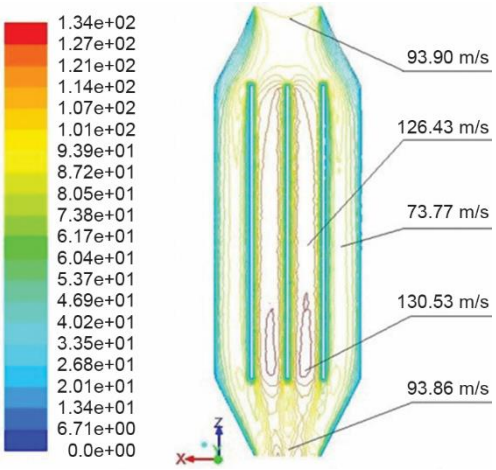

Figure 6. Middle sectional velocity of the TEG (*for color image see journal web site*)

the exhaust channels. A strong high pressure vortex zone presents in the upstream of the main pipe and gradually pushes the air-flow into the branch pipes. Through the middle two channels of exhaust acceleration, the speed reaches 130 m/s and higher when the exhaust reaches the fork export. The exhaust pressure of the middle two channels is about 5 kPa lower than that of the two outer side channels. A large backflow low pressure zone presents in the downstream of the main pipe when the exhaust flow from the branch pipes affects the main pipe. The pressure decreases by about 14.8 kPa after the contraction segment becomes confluent.

As shown in fig. 7, the exhaust temperature reduces from 593 K to 581 K along the streamwise direction due to sensible heat exhaust being absorbed by the TEG module. The temperature of the TEG fins gradually increases from 300 K to about 474 K, but the fins temperature along the axis gradually reduces, and the temperature of the transverse position of the fins remains basically the same. The temperature difference is 28 K between the fins highest and lowest temperature; meanwhile, heat is released from the TEG module to the coolant, leading to an increase in coolant temperature. Finally, the heat is released from the TEG module and the coolant to the external cooling air, leading to a temperature increase in the external cooling air. The results show that under rated power conditions, given the large engine power and exhaust volume, there is full heat exchange from the internal high temperature exhaust and fins. The fins also receive more heat, and the temperature is higher and equally distributed. Moreover, a counter-flow cooling pattern is adopted for the coupled TEG module; that is, the cooling water and exhaust flow in the opposite direction. It is possible to improve thermoelectric conversion efficiency by increasing the temperature difference.

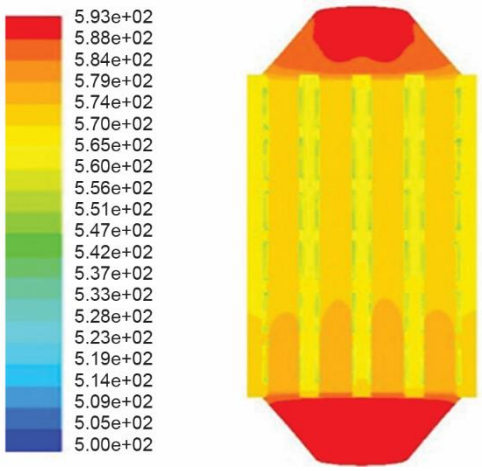

Figure 7. Outer fins temperature of the TEG
(*for color image see journal web site*)

Temperature measurement of the TEG

In this study, a displacement of a 3.168 L diesel 4-cylinder turbocharged engine is selected to test the performance of the coupled design scheme in the TEG system. It is installed in the engine exhaust muffler upstream as shown in fig. 8. The temperature measurement method in the TEG is shown in fig. 9.

As pictured in figs. 8 and 9, the engine drives the generator and changes the generator load through an external load control cabinet. A thermal insulation layer is used to bind the heat exchanger and avoid the influence of air-flow on fins heat output. High temperature exhaust flows through the TEG. The inlet and outlet temperature measurement points of the high temperature exhaust are CH1 and CH2, respectively, those of the inlet and outlet cooling water are CH3 and CH4, respectively. Three measuring points using patch-type temperature sensors are selected along the left second fin in a vertical straight line (CH5, CH6, and CH7; see fig. 3 to measure the temperature variation of the working face along the fins. The temperatures with 100% load at engine speeds of 700, 1100, 1500, 2000, 2400, 2800, and 3200 rpm are measured, and they are 543, 553, 562, 570, 578, 586, and 593 K, respectively. The data output from the

temperature sensor is automatically computer-recorded every 10 seconds to obtain the temperature of each measuring point in the heat exchanger. The mass flows of the high-temperature exhaust are respectively 0.16, 0.23, 0.30, 0.38, 0.45, 0.51, and 0.55 kg/s.

Figure 8. Diesel engine and installed positions of the TEG system

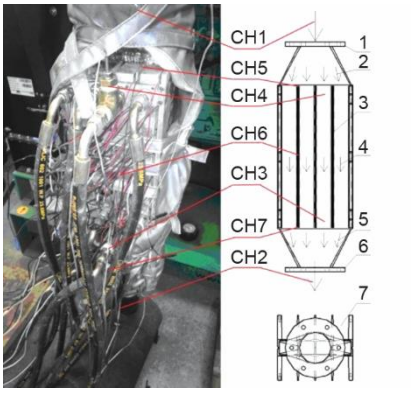

Figure 9. Experimental TEG system; *1 – inlet flange, 2 – high temperature exhaust inlet, 3 – high temperature, 4 – cooling water passage, 5 – high temperature exhaust outlet, 6 – outlet flange, 7 - shell*

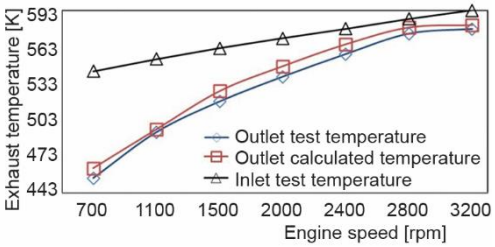

Figure 10. Temperature comparison of exhaust at different engine speeds

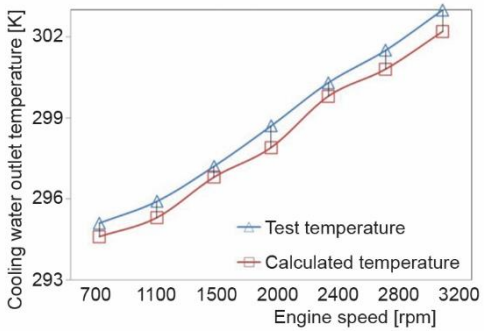

Figure 11. Cooling water outlet temperature comparison at different engine speeds

Temperature comparison of the TEG

As the engine speed increases, the temperature of the exhaust, cooling water, and fins of the TEG are shown in figs. 10-14, respectively.

Figure 10 shows a temperature comparison of exhaust at different engine speeds and fig. 11 depicts a comparison of cooling water outlet temperature at different engine speeds. Figures 12-14 show a comparison of the top, middle, and bottom temperatures of the fins at different engine speeds.

As indicated in fig. 10, the inlet and outlet temperature of the TEG increases as engine speed increases. More specifically, engine speed increases from 700 rpm to 3200 rpm, and the inlet temperature of the exhaust rises from 543 K to 593 K. The outlet temperature of exhaust increases from 455.1 K to 577.6 K, which suggests that the high temperature exhaust in the heat exchanger is reduced to differing degrees after heat dissipation. Idle speed temperature (700 rpm) is reduced by 360.9 K. The temperature is also reduced by 15.4 K under rated operating conditions (3200 rpm). In addition, the growth trends of calculation and test tem-

perature of outlet exhaust are essentially the same, although the calculation temperature is higher than the test temperature.

Figure 11 shows that the temperature of the outlet cooling water in the TEG increases approximately linearly with an increase in engine speed: the test temperature rises from 293.6 K to 303 K, the calculated temperature rises from 293.6 K to 302.2 K, and the temperature of the outlet cooling water is consistent with the experimental temperature under the corresponding engine speed. However, the calculated temperature is lower than the test temperature.

Figures 12-14 illustrate the temperature variations of the top, middle and bottom surfaces of the internal heat transfer fins, respectively.

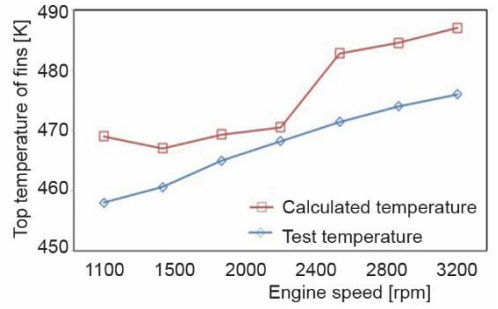

Figure 12. Top temperature comparison of fins at different engine speeds

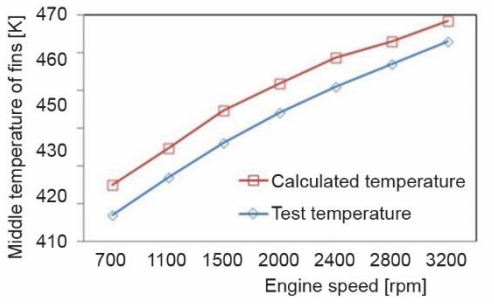

Figure 13. Middle temperature comparison of fins at different engine speeds

As shown in figs. 12-14, when the exhaust flows through the channels, the temperature of the exhaust gradually declines. The sensible exhaust heat is transferred to the internal heat transfer fins via forced convection. Temperature variations on the top, middle, and bottom of the internal heat transfer fins in the TEG system increase with increasing engine speed: the top fin temperature rises from 458 K to 476 K, the middle fin temperature increases from 417 K to 563 K, and the bottom fin temperature increases from 406 K to 449 K.

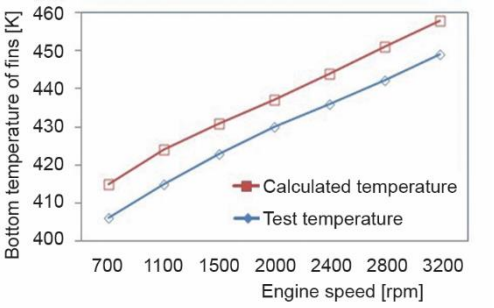

Figure 14. Bottom temperature comparison of fins at different engine speeds

At an idle speed (700 rpm), the temperature difference between the top and bottom fins reaches 52 K, presumably because the exhaust system heat transfer is too low at this speed. At the rated speed (3200 rpm), the temperature difference between the top and bottom fins is 27 K due to full heat exchange from the internal high temperature exhaust and fins. Furthermore, the exhaust temperature declines along the streamwise direction because sensible exhaust heat is absorbed by the TEG module and more heat is passed to the thermoelectric components and cooling systems. The calculated temperature increase is consistent with the test temperature of the top, middle, and bottom fins, and the temperature predicted by the code is slightly higher than the test temperature. These differences may be partially explained by the presence of

electrical contact resistances that are not accounted for because they are difficult to assess with numerical code.

According to the principle of thermoelectric conversion, the generator heat, Q_h, gains from the heat source can be displayed:

$$Q_h = \pi_{NP} I - \frac{1}{2} I^2 R + k(T_h - T_c) \tag{2}$$

where π_{NP} is the Peltier coefficient, I – the current through the thermocouple, R – the resistance, k – the thermal conductivity, T_h – the high temperature value, and T_c – the low temperature value. The first term on the right of the equation is Peltier heat; the second is Joule heat, which is determined by the transfer current, material, and structure of TEM; and the third is conductive heat, which is determined by the heat exchanger structure. Thus, TEG system performance depends on the characteristics of the TEM array and heat exchanger.

The previous simulation and test results show that when the engine changes from idle speed to rated speed, the top, middle, and bottom fin temperatures increase, respectively, from 458 K to 476 K, 417 K to 463 K, and 406 K to 449 K, while the cooling water outlet temperature increases from 293.6 K to about 303 K. Fins thermoelectric elements can therefore reach a 100 K temperature difference at all engine speeds, and the distribution is even, Thus, higher power of the coupled exhaust TEG system can be achieved by higher temperature difference, the heat transfer efficiency can be increased, and allowing for stable output performance under the coupling design of the heat exchanger and TEM array under all engine operating conditions.

Conclusions

In this work, a coupled heat transfer model of a TEG is developed, wherein the exhaust is modeled as the actual heat source with a water-cooling channel as the cold source, and convective heat transfer, heat conduction, and radiation heat transfer are solved simultaneously. Then, the established model is utilized to study the coupled relationship between high-temperature exhaust flows, structure, and the external cooling air. The main conclusions are as follows:

A heat transfer model of a TEG system coupled with high temperature exhaust, structure, and the external cooling air is established. The results show that the fins have good temperature distribution under different engine speeds. That is, the average temperature of the fins is 474 K with even distribution. The comparison of test and calculated results shows that the exhaust inlet and outlet temperature of the thermoelectric system increases with an increase in engine speed, and the cooling water outlet temperature and top, middle, and bottom fin temperatures show an approximate linear upward trend; hence, the coupled heat transfer model is validated. Moreover, the thermoelectric elements on the fins can obtain a 100 K temperature difference, the heat transfer efficiency can increase and its distribution is even, higher power of the exhaust TEG system which coupled design of the heat exchanger and TEM array can be achieved.

Acknowledgment

This work was partially supported by the National Natural Science Foundation of China (Grant No: 51375168) and Science and Technology Planning Project of Guangzhou

(2014J4100014), and the experiments were supported by the Guangzhou WANON Electric & Machine Co., Ltd.

References

[1] Chuang, Y., Chau, K. T., Thermoelectric Automotive Waste Heat Energy Recovery Using Maximum Power Point Tracking, *Energy Convers Manage, 50* (2009), 6, pp. 1506-1512
[2] Zhang, Z., *et al*. Structure of High-Power Density Thermoelectric Generator Used for Automobile[J]. *Journal of South China University of Technology: Natural Science Edition*, *40* (2012), 7, pp. 101-106
[3] Riffat, S. B., Ma, X., Thermoelectrics: A Review of Present and Potential Applications, *Appl. Therm. Eng., 23* (2003), 8, pp. 913-35
[4] Deng, Y.-D., Fan, T., Arrangement of TEG device and thermoelectric module [J], *Journal of Wuhan University of Technology, 32* (2010), 2, pp. 265-2677
[5] Du, Q.-G., *et al.,* Influence of Structure Parameters on Performance of the Thermoelectric Module [J], *Journal of Wuhan University of Technology: Materials Science, 26* (2011), 3, pp. 464-468
[6] Zhang, Z., *et al.,* Machine-Thermal Coupling Stresses Analysis of the Fin-Type Structural Thermoelectric Generator, *Journal of Electronic Materials, 46* (2017), 5, pp. 3156-3165
[7] Zhang, Y., *et al.,* Hightemperature and High-Power-Density Nanostructured Thermoelectric Generator for Automotive Waste Heat Recovery, *Energy Convers Manage, 105* (2015), Nov., pp. 946-50
[8] Liu, X., *et al.,* Performance Analysis of a Waste Heat Recovery Thermoelectric Generation System for Automotive Application, *Energy Convers Manage, 90* (2015), Jan., pp. 121-127
[9] Hsiao, Y. Y., *et al.,* A Mathematic Model of Thermoelectric Module with Applications on Waste Heat Recovery from Automobile Engine, *Energy, 35* (2010), 3, pp. 1447-1454
[10] Shtern, M., Yu., Current Trends in Improving the Efficiency of Thermoelectric Generators, *Proceedings,* IEEE Conference of Russian Young Researchers in Electrical and Electronic Engineering, ElConRus, St. Petersburg, Russia, 2019, pp. 1914-1919
[11] Guoquan, X., Investigation of Fluid-Solid Conjugate Heat Transfers for a Sedan Exhaust System, *Proceedings*, Inter. Confe. on Electric Information and Control Engineering, Wuhan, China, 2011, pp. 5076-5079
[12] Hendricks, T. J., Thermal System Interactions in Optimizing Advanced Thermoelectric Energy Recovery Systems, *Energy Resour. Technol., 129* (2007), 3, pp. 223-231
[13] Lazard, M., Heat Transfer in Thermoelectricity: Modeling, Optimization and Design, *Proceedings,* IASME/WSEAS International Conference on Heat Transfer, Thermal Engineering and Environment, HTE '09, Moscow, Russia, 2009, pp. 129-134
[14] Descombes, G., Boudigues, S., Modelling of Waste Heat Recovery for Combined Heat and Power Applications, *Applied Thermal Engineering, 29* (2009), 13, pp. 2610-2616
[15] Chen, M., *et al.,* A Three-Dimensional Numerical Model of Thermoelectric Generators in Fluid Power Systems, *International Journal of Heat and Mass Transfer, 54* (2011), 1-3, pp. 345-55
[16] Ren De-P., *et al.,* Complete Numerical Simulation of The Thermoelectric Coupling in a Thermoelectric generator, *Journal of Tsinghua University (Sci. & Tec.), 48* (2008), 8, pp. 1372-1376
[17] Zhang, Z., *et al.,* Modeling and Numerical Analysis of Internal Enhanced Direct Thermoelectric Conversion System, *Journal of South China University of Technology: Natural Science Edition,* (2011), 3, pp. 47-51
[18] Zhang, Z., Zheng, D., Numerical Research on Heat Transfer Characteristics of the Intensified Thermoelectric System for Exhaust, *Proceedings,* 4th International Conference on Intelligent Computation Technology and Automation (ICICTA2011), Washington DC, 2011, pp. 862-865
[19] Weng, C. C., Huang, M. J., A Simulation Study of Automotive Waste Heat Recovery Using a Thermoelectric Power Generator, *Int. J. Therm. Sci., 71* (2013), Sept., pp. 302-309
[20] Deng, Y. D., *et al.,* Thermal Optimization of the Heat Exchanger in an Automotive Exhaust-Based Thermoelectric Generator, *Journal of Electron Mater, 42* (2013), 7, pp. 1634-1640
[21] Hashim, H., *et al.,* Model For Geometry Optimisation Of Thermoelectric Devices In A Hybrid PV/TE System, *Renewable Energy, 87* (2016), 1, pp. 458-463
[22] He, W., *et al.,* Effects of Heat Transfer Characteristics between Fluid Channels and Thermoelectric Modules on Optimal Thermoelectric Performance, *Energy Convers Manage, 113* (2016), Apr., pp. 201-208

[23] Tian, H., *et al.,* Comparison and Parameter Optimization of a Segmented Thermoelectric Generator by using the High Temperature Exhaust of a Diesel Engine, *Energy, 84* (2015), May, pp. 121-30
[24] Royale, A., Simic, M., Research in Vehicles with Thermal Energy Recovery Systems, *Procedia Comput Sci., 60* (2015), Dec., pp. 1443-1452
[25] Meng, J. H., *et al.,* Performance Investigation and Design Optimization of a Thermoelectric Generator Applied in Automobile Exhaust Waste Heat Recovery, *Energy Convers Manage, 120* (2016), July, pp. 71-80

Paper submitted: June 8, 2019
Paper revised: July 1, 2019
Paper accepted: July 4, 2019

© 2020 Society of Thermal Engineers of Serbia.
Published by the Vinča Institute of Nuclear Sciences, Belgrade, Serbia.
This is an open access article distributed under the CC BY-NC-ND 4.0 terms and conditions.